Apical Oxidative Hyaluronan Degradation Stimulates Airway Ciliary Beating via RHAMM and RON

Dahis Manzanares, Maria-Elena Monzon, Rashmin C. Savani, and Matthias Salathe

Division of Pulmonary and Critical Care Medicine, Department of Medicine, University of Miami Miller School of Medicine, Miami, Florida; and Divisions of Pulmonary and Vascular Biology and Neonatal-Perinatal Medicine, Department of Pediatrics, University of Texas Southwestern Medical Center, Dallas, Texas

Hyaluronan (HA) is synthesized in high-molecular-weight form at the apical pole of airway epithelial cells, covering the luminal surface. When human airway epithelial cells grown and redifferentiated at the air–liquid interface (ALI) were exposed to xanthine/xanthine oxidase (X/XO), ciliary beat frequency (CBF) increased. This effect was blocked by superoxide dismutase (SOD) and catalase. Inhibition of hyaluronan synthesis inhibited the CBF response to X/XO, while addition of exogenous HA amplified it. A functionally blocking antibody to the receptor for hyaluronic acid–mediated motility (RHAMM) reduced the CBF response to X/XO. Since RHAMM has no transmembrane domain and thus cannot signal on its own, the association of RHAMM with recepteur d'origine nantais (RON), a member of the hepatocyte growth factor receptor family, was explored. Immunohistochemistry of human airway epithelium showed co-localization of RHAMM and RON at the apex of ciliated cells. Physical association of RHAMM and RON was confirmed with co-immunoprecipitations. Macrophage-stimulating protein (MSP), an agonist of RON, stimulated CBF. Genistein, a nonspecific tyrosine kinase inhibitor, and MSP β chain (β-MSP), a specific RON inhibitor, blocked the X/XO-induced CBF increase. HA present in the apical secretions of human airway epithelial cells was shown to degrade upon exposure to X/XO, a process inhibited by SOD. Low-molecular-weight HA fragments stimulated CBF, an effect blocked by anti-RHAMM antibody and genistein. These data suggest that high molecular form HA is broken down by reactive oxygen species to form low-molecular-weight fragments that signal via RHAMM and RON to stimulate CBF.

Keywords: ciliary beat frequency; hyaluronan; receptor for hyaluronan mediated motility; recepteur d'origine nantais; reactive oxygen species

CLINICAL RELEVANCE

This study provides new information on reactive oxygen species modulation of ciliary beat frequency via hyaluronan degradation and signaling by receptor for hyaluronic acid–mediated motility and recepteur d'origine nantais. Thus this research may provide information about mucociliary changes during airway inflammation.

Effective mucociliary clearance depends on adequate ciliary activity. *In vivo*, ciliary beat frequency (CBF) is regulated by the paracrine action of ATP (e.g., 1) and by hyaluronan (HA), a glycosaminoglycan present at the apex of the airway epithelium. HA, a nonsulfated polysaccharide of repeating disaccharide subunits of glucuronic acid and N-acetyl glucosamine linked by β1,4 and β1,3 glycosidic bonds, is synthesized as a high-molecular-weight molecule by three hyaluronan synthase (HAS) isoforms (2). In the airways, HA is made by airway submucosal gland cells and cells of the superficial epithelium (3, 4). Thus, it is a component of normal airway secretions (3, 5) and present on the airway surface (6).

A growing number of papers report that HA participates in signaling pathways critical for multiple cell functions. However, the molecular size is an important determinant for its biological activity (for review *see* Ref. 7). Hyaluronan < 300 kD stimulates cell proliferation and initiates signaling cascades involving inflammation (8, 9). The same molecular size of hyaluronan stimulates sperm motility (10, 11) and, as shown by us, CBF (6, 12). On the other hand, HA (> 1,000 kD) inhibits cell proliferation (13) and has been reported to have no effect on CBF (14). We have also shown that lower-molecular-weight HA stimulates ovine CBF via the receptor for hyaluronic acid mediated motility (RHAMM) or CD168 (6).

Since HA is synthesized in the airway in high-molecular-weight form, it can only signal via RHAMM after being degraded *in situ*. We have shown that the average HA size decreases after oxidative stress induced by allergen challenge in the airway lumen (15). In fact, reactive oxygen species (ROS) are potent inducers of HA depolymerization to yield smaller-sized molecules (17, 18). Thus, ROS could play a role in activating CBF via HA degradation during airway insults.

Multiple publications show that RHAMM is able to initiate signaling (for review *see* Ref. 19); however, since RHAMM does not have a transmembrane domain, the mechanisms by which signaling is achieved are poorly understood. It has been suggested that extracellular RHAMM associates with growth factor receptors such as platelet-derived growth factor receptor (PDGFR) and modifies extracellular signal–regulated kinase (ERK) signaling (20–24). ERK signaling has not been reported to modulate CBF, and most growth factor receptors in the airway are reportedly expressed at the basolateral aspect of airway epithelial cells. There is one exception, however: recepteur d'origine nantais (RON), a member of the hepatocyte growth factor receptor family and a specific receptor for macrophage-stimulating protein (MSP), has been clearly shown to be expressed at the apical membrane and to modulate CBF (25). We therefore examined whether RHAMM and RON are involved in HA-mediated CBF regulation using human airway epithelial cells grown and redifferentiated at the ALI.

(*Received in original form November 3, 2006 and in final form February 12, 2007*)

This work was partially supported by NIH grants HL-60644 and HL-67206 (to M.S.) and HL-62472 and HL-73896 (to R.C.S.) and by a James and Esther King Florida Biomedical Research Program Team Science Project Grant from the State of Florida (to M.S.).

Correspondence and requests for reprints should be addressed to Matthias Salathe, Division of Pulmonary and Critical Care Medicine, University of Miami School of Medicine, 1600 NW 10th Ave., RMSB 7063A (R-47), Miami, FL 33136. E-mail: msalathe@med.miami.edu

Am J Respir Cell Mol Biol Vol 37. pp 160–168, 2007
Originally Published in Press as DOI: 10.1165/rcmb.2006-0413OC on March 29, 2007
Internet address: www.atsjournals.org

MATERIALS AND METHODS

Materials

All media and Hank's balanced salt solution (HBSS) were purchased from Gibco, Life Technologies (Grand Island, NY). MSP and MSP β-chain (β-MSP) were obtained from R&D Systems, Inc. (Minneapolis, MN). Functionally blocking anti-RHAMM antibody (R36) has been characterized before (26). The other primary antibodies were obtained from Santa Cruz Biotechnology, Inc. (Santa Cruz, CA). Secondary antibodies were obtained from Invitrogen–Molecular Probes (Carlsbad, CA). $HA_{14\ mers}$ fragments were a generous gift from Dr. Anthony Day (Manchester, UK). Unless stated otherwise, all other materials were obtained from Sigma Chemical Company (St. Louis, MO).

Cell Culture

Human lungs were obtained from organ donors through the Life Alliance Organ Recovery Agency of the University of Miami, according to protocols approved by the local Institutional Review Board. Airway epithelial cells were isolated and frozen without expansion as described previously (27–29). For all air–liquid interface (ALI) cultures, cells were thawed, grown to confluence in a nondifferentiated state, and then trypsinized and plated onto collagen IV–coated, 24-mm Transwell-clear culture inserts as passage 1 cells (Corning Costar Corporation, Cambridge, MA) at a density of 5×10^5 cells/cm^2 in ALI media (30). After reaching confluence, the apical surface of the cells was exposed to air and used for experiments after full differentiation (about 4 wk). All *n* refer to the total number of cells studied, and all studies included cells from at least two ALI cultures from at least two different donors unless stated otherwise. All comparisons were made with date- and culture-matched cells.

Measurement of CBF and Intracellular Calcium

Cells were apically washed with PBS and placed into a special perfusion chamber allowing independent basolateral and apical perfusions. Apical and basolateral solutions were 10 mM Hepes-buffered HBSS pH 7.4 (referred to as HBSS). The cells were allowed to equilibrate at room temperature for at least 20 min before use.

Measurement of CBF was accomplished by mounting the cells onto the stage of a Nikon Eclipse E600FN upright microscope using a 60× water-immersion lens. Cells were apically perfused at 150–200 μl/min. Stopping or starting perfusion at these rates neither changed intracellular calcium nor CBF as previously reported (1, 31). Cells were imaged using infrared differential interference contrast (DIC) optics. The light path was directed to a Sony XC-7500 CCD camera acquiring images at 60 Hz, and light intensity changes due to ciliary activity were recorded and analyzed as described using our own custom-made software providing a minimal frequency resolution of 0.23 Hz and time resolution of $\sim$ 3 s (32). For a few experiments, intracellular calcium was measured using fura-2 as described before (1).

Experimental Protocols

To evaluate the effect of superoxide generation by xanthine/xanthine oxidase (X/XO) on CBF, xanthine 0.3 mM was included in the apical perfusate at all times. At the time of stimulation, either 10 μl of HBSS (control) or 10 μl of HBBS containing 100 mU/ml xanthine oxidase (treated samples) was manually added to the apical surface to allow immediate production of superoxide *in situ*, and apical perfusion was stopped for 5 min to not flush X/XO out of the system immediately. Special care was taken to avoid mechanical stimuli when adding XO (10 μl) near the corner of the chamber. Addition of HBSS alone under these conditions did not affect CBF (controls).

To evaluate the effect of oxidant scavengers on X/XO-mediated changes in CBF, catalase (800 U/ml), SOD (675 U/ml) or both were added to the xanthine-containing apical HBSS perfusate.

To inhibit HA production, 1 mM 4-methylumbelliferone (4-MU), an inhibitor of HA synthesis, was added to the basolateral media for 48 h. This dose was found to reduce new synthesis of HA by 83% in keratinocytes (33). Brief apical washes with this agent dissolved in 500 μl of PBS, pH 7.4, were performed together with media changes at 24 and 48 h. Matched controls (without 4-MU) were sham-manipulated with PBS alone. Apical washes from treated and control cells were collected for measurement of HA concentrations at 48 h by an ELISA-like, competitive assay using biotinylated HA-binding protein (34) as previously described by us (35). To evaluate the effect of exogenous HA addition on the CBF responses to X/XO, hyaluronan from *Streptococcus zooepidemicus* (100 μg/ml, final concentration) was added to the apical, xanthine-containing perfusate.

To evaluate involvement of RHAMM in the CBF response to X/XO, functionally blocking anti-RHAMM antibody (26) or control rabbit IgG (both at 25 μg/ml, final concentration) were applied apically for 30 min at 37°C before the experiment and included in the apical perfusate as described before (6).

To evaluate involvement of RON in the CBF response to X/XO, either the nonspecific tyrosine kinase inhibitor genistein (50 μM) or the specific RON inhibitor β-MSP (2–5 μg/ml) was included in the apical perfusate. Pre-incubation with these inhibitors lasted at least 15 min before XO was added.

Finally, the effect of $HA_{14\ mers}$ on CBF was evaluated. $HA_{14\ mers}$ at a final concentration of 100 μg/ml were added to the apical perfusate (without xanthine). The inhibitory effect of 50 μM genistein and 25 μg/ml blocking anti-RHAMM antibody was evaluated on CBF responses to $HA_{14\ mers}$ by pre-incubating the cells for at least 10 min before adding $HA_{14\ mers}$.

HA Degradation by ROS

To confirm that X/XO caused HA degradation under the used experimental conditions, airway epithelial cultures were treated with X/XO (0.3 mM/100 mU/ml) for 3 or 30 min or for 30 min in the presence of SOD (1,000 U/ml) and analyzed by fluorophore-assisted carbohydrate electrophoresis (FACE) as described before by Calabro and coworkers (36) and modified by us (35). Apical supernatants were collected and digested with proteinase K (125 μg/ml, 2 h at 60°C). After inactivation of the enzyme, digested samples were precipitated with 85% ethanol, and pellets were re-suspended in 0.1 M ammonium acetate, pH 7.5, and incubated overnight at 37 °C with 20 mU of chondroitinase ABC (MP Biomedicals, Solon, OH) at pH 7.5 (where hyaluronidase activity is negligible), 5 mU of keratanase (Saikagaku, Associates of Cape Code, East Falmouth, MA) and 5 mU of endo-galactosidase (Saikagaku). Hyaluronidase was omitted in order to be able to detect ROS-induced appearance of small hyaluronan fragments (35). Digested samples were ethanol-precipitated, washed, dried, derivatized with 2-aminoacridone (AMAC; Invitrogen), and run in MONO (Prozyme, San Leandro, CA) composition gels with MONO gel running buffer. After precipitation, glycosaminoglycan disaccharides (e.g., chondroitin sulfate or keratan sulfate) were expected to remain in the supernatant (35). Thus, only ethanol-precipitated HA fragments were available for derivatization with AMAC. Gels were photographed under 302 nm ultraviolet light using a ChemiDoc XRS imaging system and Quantity One analysis software (both from Bio-Rad, Hercules, CA).

To confirm changes in HA molecular weight distribution, samples were digested with proteinase K, ethanol precipitated, and electrophoresed on 0.65% SeaKem agarose (Cambrex, Rockland, ME) according to the method of Lee and Cowman (37). After transfer to a Biodyne B nylon membrane (Pall Gelman Laboratory, Ann Arbor, MI) samples were probed with b-HABP as described before (35).

Immunoprecipitation and Western Blot Analyses

Cell cultures were lysed at 4°C with 20 mM sodium phosphate, 150 mM NaCl, 5 mM EDTA, 50 mM HEPES, 1% Triton X-100, 50 mM NaF, 1 mM sodium orthovanadate, 5 mM phenylmethylsulfonyl fluoride, 10 μg/ml leupeptin, and 10 μg/ml aprotinin at pH 7.8 (lysis buffer) for 5 min. Lysed cells were centrifuged at $16{,}000 \times g$ for 5 min at 4°C to remove insoluble material. Equal amounts of total protein were taken in duplicate and immunoprecipitated with either rabbit anti-RON β-chain (2 μg/mg protein) or goat anti-RHAMM E19 (2 μg/mg protein). The samples were agitated at 4°C for 2 h. Protein A/G Plus-agarose (Santa Cruz Biotechnology) was added per manufacturer's instructions. After addition, samples were agitated for one additional hour.

For Western blotting, immunoprecipitates were recovered by centrifugation, washed with cold lysis buffer, and proteins eluted with SDS sample buffer and separated via SDS-PAGE. Proteins were electrically transferred to PVDF Immobilon-P membranes (Millipore, Bedford, MA). Membranes were blocked for 1 h at room temperature with 4%

nonfat milk diluted in 0.05% Tween-20, 50 mM Tris-HCl, 150 mM NaCl, pH 7.4. Membranes were incubated overnight at 4°C with goat anti-RHAMM E19 antibody (2 μg/ml) and developed with horseradish peroxidase (HRP)-conjugated rabbit-anti-goat antibodies. Blotting was visualized using LumiGLO, a chemiluminescent substrate (KPL, Gaithersburg, MD). Membranes were stripped using Restore Western Blot Stripping buffer (Pierce, Rockford, IL) according to the manufacturer's instructions, and rabbit anti-RON β-chain antibody (2 μg/ml) was used for blotting using the same conditions described with the anti-RHAMM antibody except that this time, HRP-conjugated goat-anti rabbit antibody was used.

Immunohistochemistry and Immunocytochemistry

Human tracheal sections obtained from organ donors were fixed with paraformaldehyde and processed according to standard procedures for immunohistochemistry. Paraffin-embedded sections were hydrated, incubated in 2 mM EDTA, pH 8.0, for 15 min at 100°C for antigen retrieval and treated with Image-iTTM FX (Invitrogen) following the manufacturer's instructions. ALI cultures were fixed with 4% paraformaldehyde and permeabilized with Triton X-100.

For both ALI cultures and tracheal sections, primary antibodies were used at the following concentrations: 4 μg/ml rabbit anti-RON β-chain, 4 μg/ml goat anti-RHAMM E19, and 10 μg/ml mouse anti-acetylated α-tubulin. Visualization was achieved using Alexa 555–labeled anti-rabbit IgG (2 μg/ml), Alexa 488–labeled anti-goat IgG (2 μg/ml), and Alexa 647–labeled anti-mouse IgG (1 μg/ml). Either rabbit or goat nonimmune IgG was used to prepare the negative control for RON β-chain and RHAMM antibodies, respectively. Nuclei were visualized with 4′6-diamidine-2-phenylindole (DAPI; Invitrogen–Molecular Probes). Samples were mounted on slides with gel/mount (Biomeda, Foster City, CA). Images were captured with a confocal laser-scanning microscope (Zeiss LSM, Thornwood, NY).

Statistics

CBF responses were compared between X/XO-challenged cultures and date and culture-matched controls. Statistical analysis was performed using JMP software from SAS Institute, Inc. (Cary, NC). Two groups were compared using Student's unpaired *t* test; one-way analysis of variance was used to compare more than two groups. A $P < 0.05$ was considered significant. If a significant difference was found by one-way analysis of variance, a group-by-group comparison was done using the Tukey-Kramer honestly significant difference test. Data were expressed as mean ± SEM.

RESULTS

Effect of X/XO on CBF

Ciliated cells grown at the ALI and apically perfused with xanthine (0.3 mM) responded to the addition of XO (100 U/ml) with an increase in CBF to a maximum of 18.8 ± 7.4% ($n = 8$) above a baseline of 5.3 ± 0.6 Hz ($P < 0.05$; $n = 8$; Figure 1E; cells from four donors responded, while cells from one other donor did not and were therefore not included in the analysis). Control cells solely exposed to buffer did not change CBF (0.3 ± 2.1% above baseline; $P > 0.05$; $n = 7$). These results were similar to studies by Yoshitsugu and colleagues (38), who found a transient CBF increase upon X/XO exposure of human maxillary sinus mucosa. In our ALI system, the initial CBF response to X/XO, if present, coincided with a $[Ca^{2+}]_i$ increase (Figures 1A and 1F, and Ref. 39), while prolonged CBF increases were dependent on HA (*see below*).

Effect of Oxidant Scavengers on CBF Response to X/XO

Initial experiments using catalase at 200 U/ml and SOD at 300 U/ml showed that these concentrations were insufficient to inhibit the CBF increase upon X/XO exposure, even though use of these scavengers at these concentrations delayed the response (data not shown). Thus, higher concentrations of the enzymes were used in an effort to inhibit the X/XO effects on CBF. Perfusion with catalase at 800 U/ml, SOD at 675 U/ml, or both inhibited the CBF increase in response to X/XO but did not affect CBF baseline before X/XO stimulation (Figures 1B–1E). These data suggest that superoxide is involved in the CBF response to X/XO.

Effect of HA Removal or Addition on CBF Increases in Response to X/XO

To evaluate the role of HA on X/XO-induced CBF responses, cell cultures were treated with 4-MU for 48 h. 4-MU has been

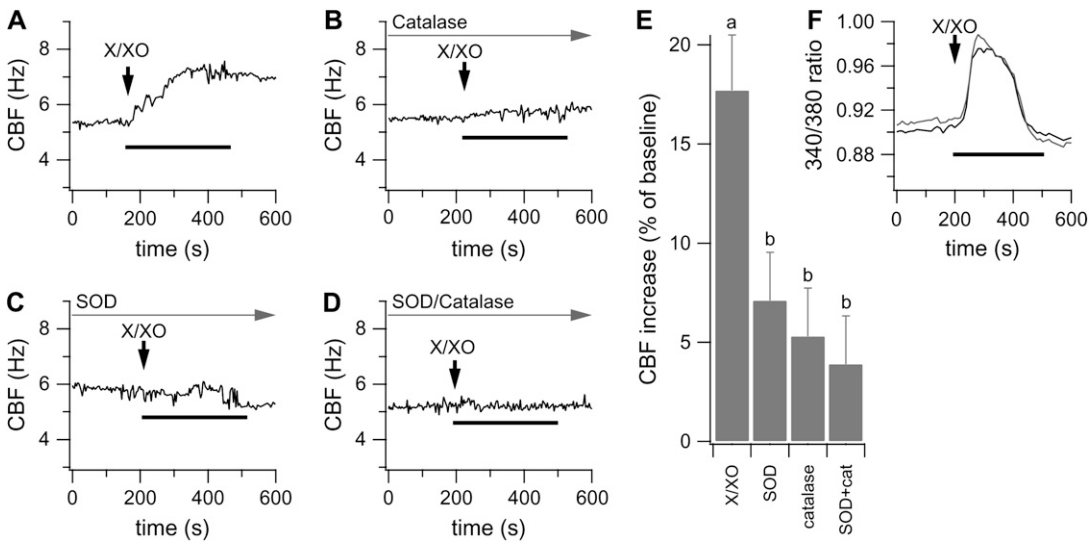

Figure 1. (A–E) Effects of xanthine (0.3 mM) and xanthine oxidase (100 mU/ml) on CBF in the presence of SOD (675 U/ml) and/or catalase (800 U/ml). *Vertical arrows* represent the time of addition of XO; *horizontal black line* represents duration (5 min) of stopping apical perfusion upon XO addition. *Gray arrows* indicate presence of catalase and/or SOD. (*E*) Quantitative analysis (all $n = 8$). Letters show levels that are significantly different (ANOVA and Tukey-Kramer): different groups are labeled with different letters while identical groups are labeled with the same letter. (*F*) Fura-2 ratiometric estimation of changes in $[Ca^{2+}]_i$: X/XO causes an initial transient $[Ca^{2+}]_i$ increase (shown are two cells).

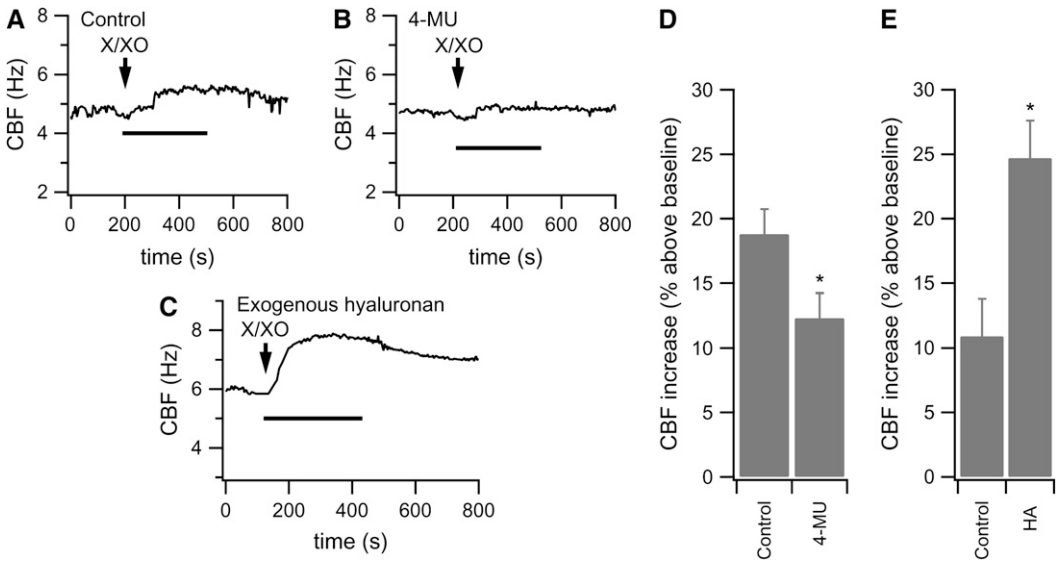

Figure 2. Effect of excess or decreased amounts of HA on CBF increase in response to X/XO. (*A*, *B*) Hyaluronan synthesis was inhibited by 4-MU for 48 h. Representative traces of control (*A*) and 4-MU–treated cells (*B*) upon exposure to X/XO (*vertical arrow*). The *line* indicates the time of stopping apical perfusion. (*C*) Exogenous high-molecular-weight HA (100 μg/ml) and X was perfused at time 0, and then XO was added (*arrow*). (*D*, *E*) Quantitative analysis of maximal CBF response to X/XO when HA synthesis was inhibited (*D*; $n = 8$) or response to excess exogenous HA (*E*; $n = 8$) compared with date- and culture-matched controls. *$P <$ 0.05 compared with control.

shown to inhibit HA synthesis in other mammalian cells (33, 40, 41). It has been proposed that 4-MU glucuronidation by endogenous UDP-glucuronyltransferases leads to UDP-glucuronic acid starvation and hyaluronan-synthesis inhibition (42). In our ALI cultures, apical HA recovered by PBS washes was 31.5 ± 4.9 ng/ml from cultures treated with 4-MU for 48 h, while the recovery from control cultures was 219.7 ± 18.5 ng/ml (each $n = 3$, $P < 0.05$). Physiologically, the CBF response to X/XO also was significantly lower in 4-MU–treated cultures than in date and culture-matched, untreated controls (each $n = 8$; Figures 2A, 2B, and 2D), indicating that HA is required for the prolonged CBF response to X/XO. Additional cultures were perfused with exogenous high molecular weight *S. zooepidemicus* HA (100 μg/ml) and exposed to X/XO as described above. Perfusion with this exogenous high-molecular-weight HA and xanthine alone for 5 min before XO addition did not influence baseline CBF (data not shown). However, inclusion of HA potentiated the CBF response to X/XO significantly, suggesting that oxidant-induced HA degradation provided smaller fragments that stimulated CBF ($n = 8$; Figures 2C and 2E). Furthermore, the CBF increase lasted significantly longer than in control cells in four out of eight cells treated. Therefore, addition or depletion of HA modulates the response to X/XO.

Effect of Functionally Blocking Anti-RHAMM Antibody on the CBF Response to X/XO

We previously showed that HA-stimulated ovine CBF responses occur via RHAMM (6), an HA receptor that also is expressed at the apex of human airway epithelial cells and ALI cultures (*see below*). When human cells cultured at the ALI were pre-incubated with a functionally blocking anti-RHAMM antibody (26), baseline CBF did not change ($n = 4$). However, these antibodies significantly reduced the highest CBF response within 5 min (maximal) and CBF at 5 min after exposure to X/XO was reduced compared with control cultures pre-incubated with a nonspecific IgG (Figures 3A–3C). Blocking RHAMM caused the CBF response to X/XO to decrease below baseline after an initial short increase, when compared with rabbit IgG treatment (Figure 3). These data therefore suggest that maximal and prolonged X/XO-mediated CBF increases are due to HA breakdown products binding to and signaling through RHAMM.

Involvement of RON in the CBF Response to X/XO

RHAMM does not have a trans-membrane domain, and the manner in which RHAMM signals is poorly understood. Cooperation with growth factor receptors has been implicated. Since RON,

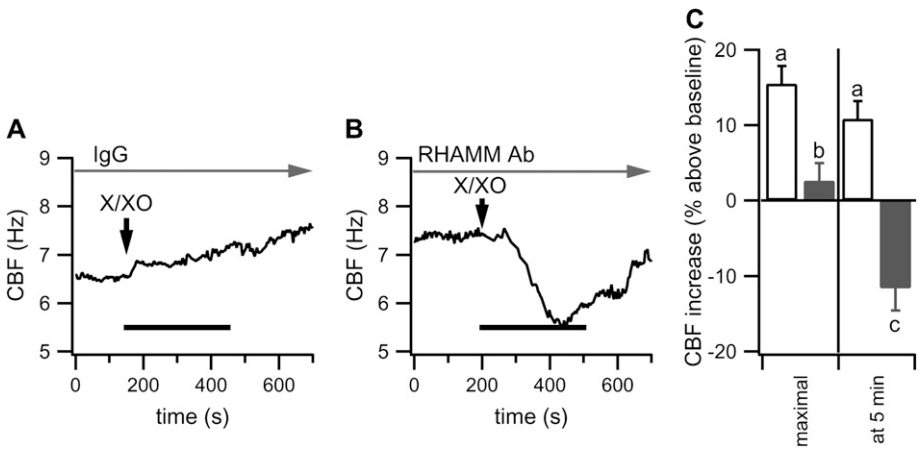

Figure 3. Effect of functionally blocking RHAMM antibody on CBF response to X/XO. Cells were incubated for 30 min at 37°C with rabbit IgG (25 μg/ml) or RHAMM antibody (25 μg/ml). Representative responses to X/XO are shown in the presence of control IgG (*A*) or anti-RHAMM Ab (*B*). *Vertical arrow* and *black lines* used as in other figures. *Gray arrows* indicate presence of IgG/RHAMM antibodies (*C*) Quantitative analysis of maximal CBF increase and CBF increase at 5 min after X/XO ($n = 4$ in each group). Letters show levels that are significantly different (ANOVA and Tukey-Kramer): different groups are labeled with different letters while identical groups are labeled with the same letter.

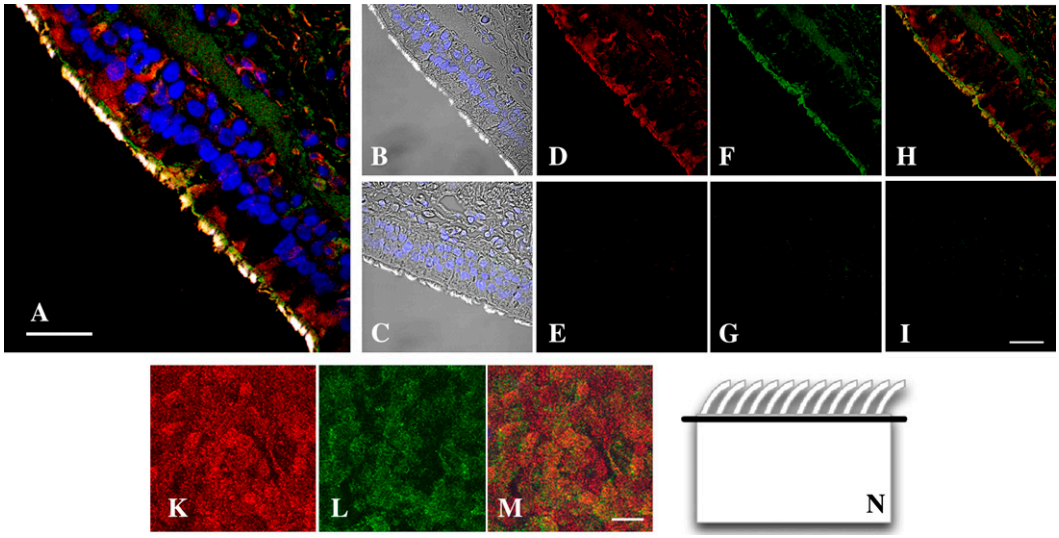

Figure 4. Expression of RON and RHAMM at the apical membrane of human airway epithelia. (*A–I*) Tracheal section: (*A*) Merged image shows all channels including anti-RON β-chain (secondary with Alexa 555, pseudocolored *red*), anti-RHAMM (E19; secondary with Alexa 488; pseudocolored *green*), and acetylated α-tubulin antibody (secondary with Alexa 647, pseudocolored *white*). Nuclei labeled with DAPI (pseudocolored *blue*). *Bar* = 20 μm. (*B* and *C*) DIC images with acetylated α-tubulin and DAPI staining, (*D* and *E*) RON β-chain staining; (*F* and *G*) RHAMM staining; (*H* and *I*) show both RON β-chain and RHAMM staining. (*E*, *G*, and *I*) Images from non-immune controls for RON and RHAMM antibodies. (*H*) Co-localization of RHAMM and RON at the apex. *Bar* = 20 μm. (*K–M*) Apical confocal section through an ALI culture stained for RON β-chain (pseudocolored *red*), RHAMM (pseudocolored *green*), and a merged image showing co-localization at the apex. *Bar* = 10 μm. (*N*) Cartoon indicating the level of the confocal section taken from an ALI culture for images *K–M*.

a hepatocyte growth factor receptor family member, is the only growth factor receptor known to be expressed apically in airway epithelial cells (25), the role of RON in X/XO-mediated CBF modulation by hyaluronan was examined.

Expression of RON and RHAMM was confirmed in epithelial cells of human tracheal sections (Figure 4), where RON and RHAMM co-localized apically (Figures 4A and 4H). Immunocytochemistry performed in ALI cell cultures also demonstrated expression and co-localization of RHAMM and RON at the apex (Figures 4K–4M). Cultures from three different donors were examined and revealed the same result.

To examine a physical interaction between RHAMM and RON, co-immunoprecipitation experiments were executed. As shown in Figure 5, immunoprecipitation of cell lysates with a RON antibody co-precipitated RHAMM. The RHAMM immunopositive band was seen at 95 kD. Although less efficient, immunoprecipitation with RHAMM antibody also recovered RON in the precipitate. The same results were obtained in three independent experiments using cells from different donors. Put together, these results indicate not only that both proteins are in a position to interact with each other but also that a fraction of RON and RHAMM interact so that they can be immunoprecipitated.

Next, the influence of the natural activator of RON, macrophage stimulating protein (MSP), on ciliary activity was confirmed as previously shown (25): cilia in ALI cultures also responded to MSP in a concentration-dependent manner (Figure 6).

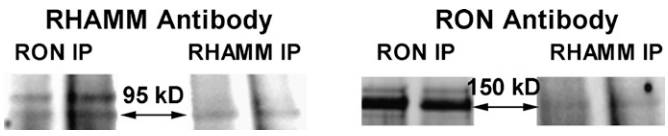

Figure 5. Immunoprecipitation of ALI cell culture extracts shows RON/RHAMM interaction. *Left panel*: RHAMM (95 kD) is detected by Western after immunoprecipitation (IP) with RON or RHAMM antibodies (higher-molecular-weight band is nonspecific). *Right panel*: RON (150-kD β-chain) is detected by Western after IP with RON or RHAMM antibodies. The level of RON and RHAMM after RHAMM IP cannot be compared due to different exposure times of chemiluminescence (*duplicate lanes*).

In order to examine the role of RON in X/XO-mediated CBF modulation by HA, a specific RON inhibitor, β-MSP, was used. β-MSP binds to RON but prevents activation (43). β-MSP (5 μg/ml) inhibited the calcium-independent, prolonged CBF increase in response to X/XO (n = 4; Figure 7). The same was true for the general tyrosine kinase inhibitor genistein (50 μM; n = 4; Figure 7). In the presence of both inhibitors, X/XO significantly decreased CBF below original baseline, consistent with previous data in the literature reporting a decrease in CBF to ROS if apical HA was absent due to extensive washing or use of detached cells (e.g., 44–46). These data suggest that RON plays an active role in the calcium-independent, prolonged CBF increase in response to X/XO.

Degradation of Apical Hyaluronan by X/XO

To confirm that the X/XO response involves HA breakdown, we studied the effect of X/XO on the apical HA size in ALI cultures using FACE. By the appropriate use of enzymes and ethanol precipitation, only HA fragments remain in the sample to react with the fluorescent marker, allowing sensitive detection of HA degradation products (Figure 8). Consistent with the CBF data, increased amounts of HA fragments were detected within 3 min of X/XO exposure. Degradation was inhibited by SOD. A similar approach to demonstrate the degradation of HA has been used before by our group (35). Parallel experiments using biotinylated HA binding protein to detect HA also indicated changes in HA molecular weight distribution that are inhibited by SOD (data no shown).

Effect of Low-Molecular-Weight HA on CBF

Once it was shown that HA degradation occurred under the conditions of our experiments, we used $HA_{14\text{-mers}}$ (corresponding to 7 disaccharides repeats with a mass of 2,673 Da) to evaluate if low-molecular-weight HA could mediate the effect of oxidative HA degradation on CBF. The size of $HA_{14\text{-mers}}$ is large enough to interact with most of the known HA-binding proteins (requires at least 6 mers), and the molecular weight is within the

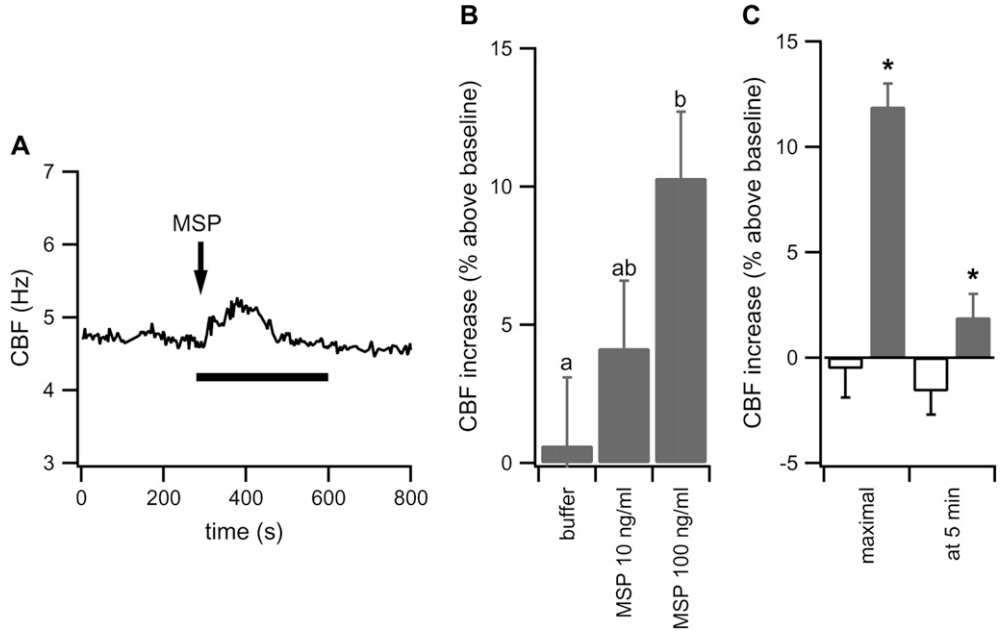

Figure 6. Effect of human recombinant MSP on CBF. (*A*) Representative CBF trace upon apical stimulation with 100 ng/ml MSP. Arrow and line used as in previous figures. (*B*) Analysis of maximal CBF increase at two different MSP concentrations (each $n = 4$). Letters show levels that are significantly different (ANOVA and Tukey-Kramer): different groups are labeled with different letters, while identical groups are labeled with the same letter. (*C*) Analysis of maximal CBF increase and increase at 5 min in the presence of 100 ng/ml MSP (*solid bars*) versus controls not exposed to MSP (*open bars*); $n = 4$ in each group, $^*P < 0.05$ compared with control.

range that has been associated with signaling (7). Also, viscosity of the sample is low enough to allow addition with a final concentration of 100 μg/ml in conditions similar to the X/XO experiments.

In control experiments using 100 μg/ml umbilical cord hyaluronan with a molecular size over 500 kD, CBF did not change significantly: perfusion with umbilical cord HA did not increase CBF significantly above buffer perfusion alone (CBF increase of 5.6 ± 2.1% above a baseline of 7.2 ± 0.2 Hz for umbilical cord HA, n = 20, versus 3.0 ± 2.3% above a baseline of 7.2 ± 0.2 Hz for buffer, $n = 18$; $P > 0.05$). On the other hand, $HA_{14\ mers}$ stimulated CBF in four of six cells tested (one in each of two ALI cultures) by 26 ± 2.6% above baseline when all cells were included in the analysis or by 34.8 ± 2.8% if only the four responding cells were included (Figure 9). The percentage of cells responding to hyaluronan corresponds to our previous experience (6, 12). The CBF responses to $HA_{14\text{-}mers}$ were usually delayed, possibly due to the lack of an initial Ca^{2+} transient likely caused by ROS and not HA. Genistein (50 μM) inhibited the CBF response to $HA_{14\text{-}mers}$, as did 25 μg/ml functionally blocking anti-RHAMM antibody (Figure 9). These data suggest that HA binds to RHAMM to activate a tyrosine kinase, most likely RON, that mediates the changes in CBF (Figure 10).

DISCUSSION

Previous work in our laboratory demonstrated that submerged cultures from ovine epithelial cells respond to HA with an increase in CBF that is mediated by RHAMM (6). The present work examined the possibility that HA degradation and signaling could act as a stimulus for CBF in human airway epithelial cells cultured at the ALI. We used xanthine/xanthine oxidase

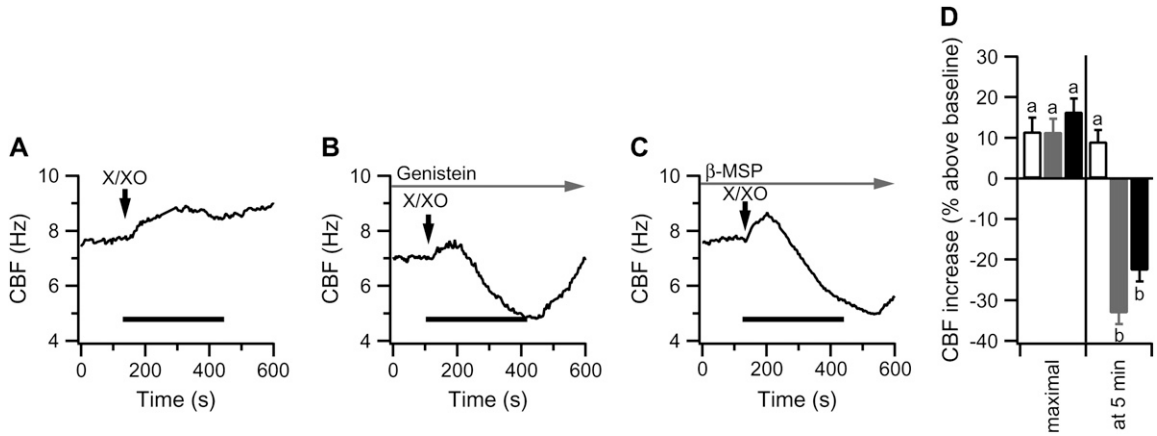

Figure 7. Effect of genistein and the functionally blocking β-MSP on CBF in response to X/XO. (*A*) Control cells exposed to X/XO as described. *Arrows* and *lines* used as in previous figures. (*B*) Cultures exposed to X/XO in the presence of 50 μM genistein or (*C*) 5 μg/ml β-MSP. (*D*) Analysis of maximal and sustained CBF increases (5 min); $n = 4$ in each group. *Open bar*, control; *shaded bar*, genistein; *solid bar*, β-MSP. Letters show levels that are significantly different (ANOVA and Tukey-Kramer): different groups are labeled with different letters, while identical groups are labeled with the same letter.

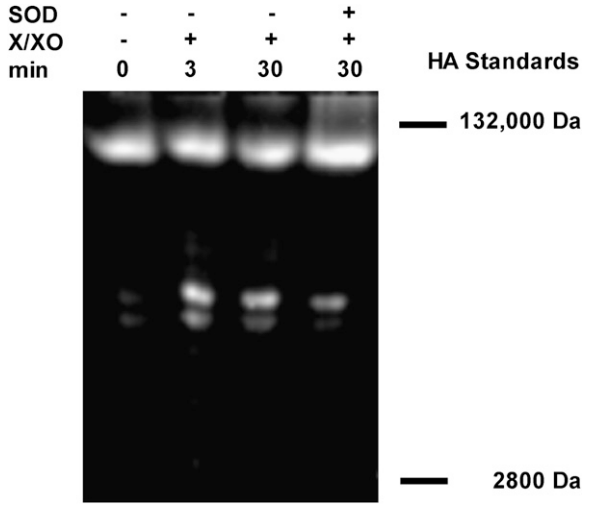

Figure 8. Time course of HA degradation upon apical exposure to X/XO in ALI cultures. A small amount of depolymerized HA (here seemingly running at ~ 15,000–20,000 Da) is seen in the control lane, but the amount increased within the first 3 min of X/XO exposure (image representative of three separate experiments). Treatment with superoxide dismutase partially prevented X/XO-induced HA degradation. Note: Correct identification of the HA fragment size is complicated by the reported anomalous behavior of small HA fragments on these gels and the potential effect of the chemical changes induced by oxidation.

(X/XO) as the source of ROS because previous work had indicated that X/XO was able to stimulate CBF in sinus mucosal tissues that was likely also covered with HA (38).

X/XO produces superoxide and derived free radicals. Superoxide spontaneously dismutates to hydrogen peroxide, but also is able to react with nitric oxide to form peroxynitrite. In the presence of metals such as iron and copper, hydrogen peroxide produced by spontaneous superoxide dismutation can convert to hydroxyl radicals, and this reaction is accelerated by the presence of superoxide. Which radical is responsible for the observed changes in CBF is difficult to decipher, as the large concentrations of catalase and SOD needed to inhibit the CBF response prevents distinction between superoxide and hydroxyl radicals. For the data presented here, however, this issue is not critical, as the results show that the signaling initiated by these radicals include both an increase in $[Ca^{2+}]_i$ and signaling via degradation products of HA. In this context, H_2O_2 is unlikely a significant contributor as H_2O_2 at the expected concentrations neither causes HA degradation (47) nor $[Ca^{2+}]_i$ increases in bovine airway epithelia (39).

Increases in $[Ca^{2+}]_i$ are well known to stimulate CBF (e.g., 32, 48). Consistent with our findings, X/XO has been found to increase $[Ca^{2+}]_i$, an effect blocked by antioxidants (39, 49, 50). In bovine tracheal epithelia, hypoxanthine/XO increased $[Ca^{2+}]_i$ within 3 min, an effect proportional to the XO concentration used (39). These findings are consistent with our results showing that X/XO initially increases $[Ca^{2+}]_i$, temporally related with the initial CBF increase in human airway epithelial cells (Figure 1). However, transient $[Ca^{2+}]_i$ increases did not explain the prolonged CBF increase observed upon X/XO exposure.

The presence of HA at the apex of polarized airway epithelial cells clearly modifies the CBF response to ROS. As shown here, high-molecular-weight HA, produced by airway epithelial cells, is not able to modify CBF. When cells were exposed to ROS in the presence of excess high-molecular-weight HA, however, the CBF response to X/XO was potentiated. On the other hand, CBF responses to X/XO were diminished after suppression of HA synthesis by 4-MU (Figure 2B). These data suggest that HA breakdown products were involved in modulating CBF. In support of this hypothesis, degradation of HA occurs in the cells as early as 3 min after X/XO addition, as shown by FACE.

It is known that the size of HA is critical for its biological activity. HA < 300 kD has been demonstrated to stimulate cell proliferation and to initiate signaling cascades involving inflammation (8, 9). The same molecular size of HA has been shown to stimulate sperm motility (10, 11) and CBF as shown here and by us before (6, 12). On the other hand, higher-molecular-weight HA (> 1,000 kD) inhibits cell proliferation (13) and has no effect on CBF (14).

High concentrations of radicals have been reported to decrease CBF (e.g., 44–46). Even at more physiological concentrations (≥ 10 μM), hydrogen peroxide (H_2O_2) reduced CBF without having a significant cytotoxic effect (51, 52). Although H_2O_2 can degrade HA, this occurs at high concentrations and usually is not seen when H_2O_2 is applied in biological systems (47). Furthermore, most of the reported experiments used brushed

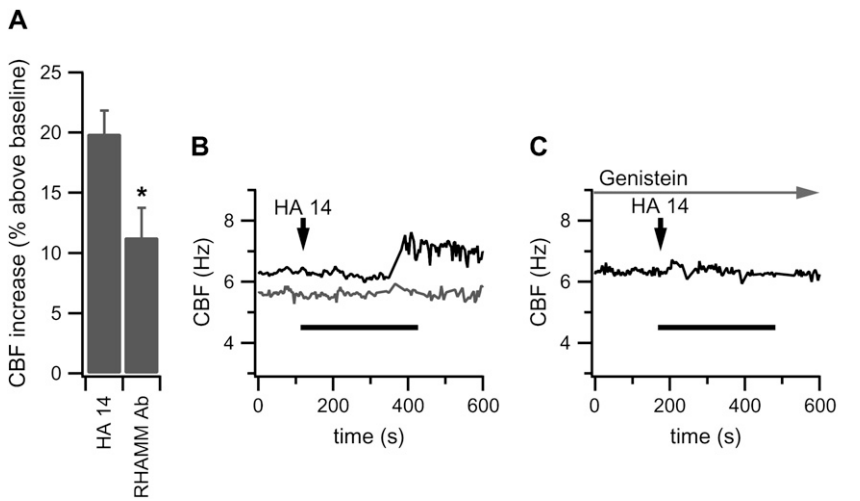

Figure 9. CBF responses to $HA_{14\text{-mers}}$ (100 μg/ml). (*A*) Quantitative analysis of maximal CBF response of cells stimulated by $HA_{14\text{-mers}}$ in the presence of control IgG (labeled HA 14) or functionally blocking RHAMM antibodies ($n = 4$ for each group). (*B*) Two different cells shown, one with and one without a response to $HA_{14\text{-mers}}$ (4 out of 6 cells responded). (*C*) All cells failed to respond to $HA_{14\text{-mers}}$ in the presence of genistein 50 μM. *Arrows* and *lines* used as in other figures. (*D*) Quantitative analysis of maximal CBF response of cells stimulated by $HA_{14\text{-mers}}$ in the presence or absence of genistein ($n = 4$ responding cells for each group). *$P < 0.05$ compared with $HA_{14\text{-mers}}$ controls.

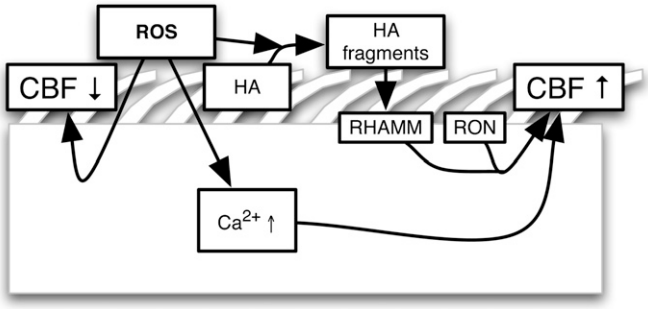

Figure 10. Working model showing the action of ROS on airway epithelial cells mediated by the degradation of HA. The direct action of ROS on CBF and intracellular calcium is also depicted. Degradation of apical high-molecular-weight HA by ROS generates fragments that trigger a signal through RHAMM and RON for a sustained increase of CBF.

cells or tissue culture methods that result in spare cells attached to support surfaces and a lack of HA. One report, however, showed that in cultured cell layers that likely contained HA on their surfaces, exposure to low concentrations of superoxide radicals actually increased CBF (38).

The CBF response to X/XO was inhibited with functionally blocking anti-RHAMM antibody. These data implicate RHAMM, a receptor known to signal upon HA degradation. Hyaluronan has been shown to increase sperm motility and sperm velocity *in vitro* (10, 53), an effect mediated by RHAMM that is expressed along the sperm tail (54). Despite good evidence of cell surface localization and multiple publications showing that signaling occurs through RHAMM (for review *see* Ref. 19), RHAMM surprisingly does not contain an apparent transmembrane domain. The mechanisms by which this signaling is therefore achieved are poorly understood. It has been suggested that extracellular RHAMM associates with growth factor receptors such as PDGFR and modifies ERK signaling (20–22).

If RHAMM signals through a growth factor receptor to stimulate CBF, it is important to know which growth factor receptors are expressed at the apex of human airway epithelia. Epidermal growth factor receptor (EGFR) is expressed basolaterally (16). PDGFR also is expressed (55), but it is not clear that apical expression occurs. RON, however, is clearly localized to the apical membrane (25) and stimulation of RON has been previously shown to increase CBF *in vitro* (25). Here, we demonstrate both polarized expression of RON and RHAMM in airway sections and ALI cultures of human airway epithelial cells, in agreement with our hypothesis showing co-localization at the apex. Furthermore, we demonstrate that both receptors interact as they can be by co-immunoprecipitated using an antibody against either protein. In addition, we confirmed CBF stimulation with the RON agonist MSP. CBF responses to X/XO were inhibited not only with the functionally blocking anti-RHAMM antibody but also with the RON antagonist β-MSP. Furthermore, the tyrosine kinase inhibitor genistein blocked both the CBF response to X/XO and the CBF response to small hyaluronan fragments. These data therefore suggest that HA degradation by X/XO stimulates RHAMM and RON and that the combined action stimulates CBF.

In summary, the presented data show that CBF increases upon exposure of fully differentiated airway epithelial cells to X/XO both by an initial increase in $[Ca^{2+}]_i$ and by a signal stemming from HA breakdown products that signal via RHAMM and RON, possibly in sequence (Figure 10). However, an additional co-signal that stimulates RON cannot be completely excluded. The details of the RHAMM–RON interaction and the intracellular signal transduction mechanisms by RON activation to stimulate CBF remain to be elucidated.

Conflict of Interest Statement: None of the authors has a financial relationship with a commercial entity that has an interest in the subject of this manuscript.

Acknowledgments: The authors thank Drs. G. Conner and R. Forteza for helpful advice and Dr. Anthony Day for the hyaluronan fragments. They also thank Nathalie Schmidt and Drs. Z. Sutto and A. Schmid for technical advice. Microscopic images were acquired at the University of Miami Analytical Imaging Core Facility.

References

1. Lieb T, Wijkstrom Frei C, Frohock JI, Bookman RJ, Salathe M. Prolonged increase in ciliary beat frequency after short-term purinergic stimulation in human airway epithelial cells. *J Physiol* 2002;538:633–646.
2. Weigel PH, Hascall VC, Tammi M. Hyaluronan synthases. *J Biol Chem* 1997;272:13997–14000.
3. Basbaum CB, Finkbeiner WE. Airway secretion: a cell-specific analysis. *Horm Metab Res* 1988;20:661–667.
4. Paul A, Picard J, Mergey M, Veissiere D, Finkbeiner WE, Basbaum CB. Glycoconjugates secreted by bovine tracheal serous cells in culture. *Arch Biochem Biophys* 1988;260:75–84.
5. Baraniuk JN, Shizari T, Sabol M, Ali M, Underhill CB. Hyaluronan is exocytosed from serous, but not mucous cells, of human nasal and tracheobronchial submucosal glands. *J Investig Med* 1996;44:47–52.
6. Forteza R, Lieb T, Aoki T, Savani RC, Conner GE, Salathe M. Hyaluronan serves a novel role in airway mucosal host defense. *FASEB J* 2001;15:2179–2186.
7. Stern R, Asari AA, Sugahara KN. Hyaluronan fragments: an information-rich system. *Eur J Cell Biol* 2006;85:699–715.
8. Horton MR, Olman MA, Bao C, White KE, Choi AM, Chin BY, Noble PW, Lowenstein CJ. Regulation of plasminogen activator inhibitor-1 and urokinase by hyaluronan fragments in mouse macrophages. *Am J Physiol Lung Cell Mol Physiol* 2000;279:L707–L715.
9. Horton MR, Shapiro S, Bao C, Lowenstein CJ, Noble PW. Induction and regulation of macrophage metalloelastase by hyaluronan fragments in mouse macrophages. *J Immunol* 1999;162:4171–4176.
10. Sbracia M, Grasso J, Sayme N, Stronk J, Huszar G. Hyaluronic acid substantially increases the retention of motility in cryopreserved/thawed human spermatozoa. *Hum Reprod* 1997;12:1949–1954.
11. Ranganathan S, Bharadwaj A, Datta K. Hyaluronan mediates sperm motility by enhancing phosphorylation of proteins including hyaluronan binding protein. *Cell Mol Biol Res* 1995;41:467–476.
12. Lieb T, Forteza R, Salathe M. Hyaluronic acid in cultured ovine tracheal cells and its effect on ciliary beat frequency. *J Aerosol Med* 2000;13:231–237.
13. Delpech B, Girard N, Bertrand P, Courel MN, Chauzy C, Delpech A. Hyaluronan: fundamental principles and applications in cancer. *J Intern Med* 1997;242:41–48.
14. Morimoto K, Yamaguchi H, Iwakura Y, Morisaka K, Ohashi Y, Nakai Y. Effects of viscous hyaluronate-sodium solutions on the nasal absorption of vasopressin and an analogue. *Pharm Res* 1991;8:471–474.
15. Forteza RM, Conner GE, Salathe M. Hyaluronan in the airways. In: Garg HG, Hales CA, editors. Chemistry and biology of hyaluronan. Amsterdam: Elsevier Ltd.; 2004. pp. 323–337.
16. Polosa R, Prosperini G, Leir SH, Holgate ST, Lackie PM, Davies DE. Expression of c-erbB receptors and ligands in human bronchial mucosa. *Am J Respir Cell Mol Biol* 1999;20:914–923.
17. Mapp PI, Grootveld MC, Blake DR. Hypoxia, oxidative stress and rheumatoid arthritis. *Br Med Bull* 1995;51:419–436.
18. Frati E, Khatib AM, Front P, Panasyuk A, Aprile F, Mitrovic DR. Degradation of hyaluronic acid by photosensitized riboflavin in vitro: modulation of the effect by transition metals, radical quenchers, and metal chelators. *Free Radic Biol Med* 1997;22:1139–1144.
19. Turley EA, Harrison R. RHAMM, a member of the hyaladherins. In: Hascall VC, Yanagishita M, editors. Science of hyaluronan today. http://www.glycoforum.gr.jp/science/hyaluronan/HA11/HA11E.html (accessed November 1, 2006).
20. Cheung WF, Cruz TF, Turley EA. Receptor for hyaluronan-mediated motility (RHAMM), a hyaladherin that regulates cell responses to growth factors. *Biochem Soc Trans* 1999;27:135–142.

21. Wang C, Thor AD, Moore DH II, Zhao Y, Kerschmann R, Stern R, Watson PH, Turley EA. The overexpression of RHAMM, a hyaluronan-binding protein that regulates ras signaling, correlates with overexpression of mitogen-activated protein kinase and is a significant parameter in breast cancer progression. *Clin Cancer Res* 1998;4:567–576.
22. Zhang S, Chang MC, Zylka D, Turley S, Harrison R, Turley EA. The hyaluronan receptor RHAMM regulates extracellular-regulated kinase. *J Biol Chem* 1998;273:11342–11348.
23. Lynn BD, Li X, Cattini PA, Nagy JI. Sequence, protein expression and extracellular-regulated kinase association of the hyaladherin RHAMM (receptor for hyaluronan mediated motility) in PC12 cells. *Neurosci Lett* 2001;306:49–52.
24. Turley EA, Noble PW, Bourguignon LY. Signaling properties of hyaluronan receptors. *J Biol Chem* 2002;277:4589–4592.
25. Sakamoto O, Iwama A, Amitani R, Takehara T, Yamaguchi N, Yamamoto T, Masuyama K, Yamanaka T, Ando M, Suda T. Role of macrophage-stimulating protein and its receptor, RON tyrosine kinase, in ciliary motility. *J Clin Invest* 1997;99:701–709.
26. Savani RC, Wang C, Yang B, Zhang S, Kinsella MG, Wight TN, Stern R, Nance DM, Turley EA. Migration of bovine aortic smooth muscle cells after wounding injury: the role of hyaluronan and RHAMM. *J Clin Invest* 1995;95:1158–1168.
27. Fragoso MA, Fernandez V, Forteza R, Randell SH, Salathe M, Conner GE. Transcellular thiocyanate transport by human airway epithelia. *J Physiol* 2004;561:183–194.
28. Nlend MC, Bookman RJ, Conner GE, Salathe M. Regulator of G-protein signaling protein 2 modulates purinergic calcium and ciliary beat frequency responses in airway epithelia. *Am J Respir Cell Mol Biol* 2002; 27:436–445.
29. Schmid A, Bai G, Schmid N, Zaccolo M, Ostrowski L, Conner G, Fregien N, Salathe M. Real-time analysis of cAMP-mediated regulation of ciliary motility in single primary human airway epithelial cells. *J Cell Sci* 2006;119:4176–4186.
30. Fulcher ML, Gabriel S, Burns KA, Yankaskas JR, Randell SH. Well-differentiated human airway epithelial cell cultures. *Methods Mol Med* 2005;107:183–206.
31. Sutto Z, Conner GE, Salathe M. Regulation of human airway ciliary beat frequency by intracellular pH. *J Physiol* 2004;560:519–532.
32. Salathe M, Bookman RJ. Mode of Ca^{2+} action on ciliary beat frequency in single ovine airway epithelial cells. *J Physiol* 1999;520:851–865.
33. Rilla K, Pasonen-Seppanen S, Rieppo J, Tammi M, Tammi R. The hyaluronan synthesis inhibitor 4-methylumbelliferone prevents keratinocyte activation and epidermal hyperproliferation induced by epidermal growth factor. *J Invest Dermatol* 2004;123:708–714.
34. Bray BA, Hsu W, Turino GM. Lung hyaluronan as assayed with a biotinylated hyaluronan-binding protein. *Exp Lung Res* 1994;20:317–330.
35. Casalino-Matsuda SM, Monzon ME, Conner GE, Salathe M, Forteza RM. Role of hyaluronan and reactive oxygen species in tissue kallikrein-mediated epidermal growth factor receptor activation in human airways. *J Biol Chem* 2004;279:21606–21616.
36. Calabro A, Hascall VC, Midura RJ. Adaptation of FACE methodology for microanalysis of total hyaluronan and chondroitin sulfate composition from cartilage. *Glycobiology* 2000;10:283–293.
37. Lee HG, Cowman MK. An agarose gel electrophoretic method for analysis of hyaluronan molecular weight distribution. *Anal Biochem* 1994; 219:278–287.
38. Yoshitsugu M, Matsunaga S, Hanamure Y, Rautiainen M, Ueno K, Miyanohara T, Furuta S, Fukuda K, Ohyama M. Effects of oxygen radicals on ciliary motility in cultured human respiratory epithelial cells. *Auris Nasus Larynx* 1995;22:178–185.
39. Kanoh S, Kondo M, Tamaoki J, Kobayashi H, Motoyoshi K, Nagai A. Effects of reactive oxygen species on intracellular calcium in bovine tracheal epithelium: modulation by nitric oxide. *Exp Lung Res* 2000; 26:335–348.
40. Nakamura T, Takagaki K, Shibata S, Tanaka K, Higuchi T, Endo M. Hyaluronic-acid-deficient extracellular matrix induced by addition of 4-methylumbelliferone to the medium of cultured human skin fibroblasts. *Biochem Biophys Res Commun* 1995;208:470–475.
41. Kosaki R, Watanabe K, Yamaguchi Y. Overproduction of hyaluronan by expression of the hyaluronan synthase Has2 enhances anchorage-independent growth and tumorigenicity. *Cancer Res* 1999;59:1141–1145.
42. Kakizaki I, Kojima K, Takagaki K, Endo M, Kannagi R, Ito M, Maruo Y, Sato H, Yasuda T, Mita S, *et al.* A novel mechanism for the inhibition of hyaluronan biosynthesis by 4-methylumbelliferone. *J Biol Chem* 2004;279:33281–33289.
43. Wang MH, Julian FM, Breathnach R, Godowski PJ, Takehara T, Yoshikawa W, Hagiya M, Leonard EJ. Macrophage stimulating protein (MSP) binds to its receptor via the MSP beta chain. *J Biol Chem* 1997;272: 16999–17004.
44. Min YG, Ohyama M, Lee KS, Rhee CS, Oh SH, Sung MW, Yun JB, Jung IH. Effects of free radicals on ciliary movement in the human nasal epithelial cells. *Auris Nasus Larynx* 1999;26:159–163.
45. Burman WJ, Martin WJ II. Oxidant-mediated ciliary dysfunction: possible role in airway disease. *Chest* 1986;89:410–413.
46. Kantar A, Oggiano N, Giorgi PL, Braga PC, Fiorini R. Polymorphonuclear leukocyte-generated oxygen metabolites decrease beat frequency of human respiratory cilia. *Lung* 1994;172:215–222.
47. Adler KB, Holden-Stauffer WJ, Repine JE. Oxygen metabolites stimulate release of high-molecular-weight glycoconjugates by cell and organ cultures of rodent respiratory epithelium via an arachidonic acid-dependent mechanism. *J Clin Invest* 1990;85:75–85.
48. Zhang L, Sanderson MJ. The role of cGMP in the regulation of rabbit airway ciliary beat frequency. *J Physiol* 2003;551:765–776.
49. Volk T, Hensel M, Kox WJ. Transient Ca^{2+} changes in endothelial cells induced by low doses of reactive oxygen species: role of hydrogen peroxide. *Mol Cell Biochem* 1997;171:11–21.
50. Az-ma T, Saeki N, Yuge O. Cytosolic Ca^{2+} movements of endothelial cells exposed to reactive oxygen intermediates: role of hydroxyl radical-mediated redox alteration of cell-membrane Ca2+ channels. *Br J Pharmacol* 1999;126:1462–1470.
51. Jackowski JT, Szepfalusi ZS, Wanner DA, Seybold ZV, Sielczak MW, Lauredo IT, Adams T, Abraham WM, Wanner A. Effects of P. aeruginosa-derived bacterial products on tracheal ciliary function: role of O_2 radicals. *Am J Physiol* 1991;260:L61–L67.
52. Kobayashi K, Salathe M, Pratt MM, Cartagena NJ, Soloni F, Seybold ZV, Wanner A. Mechanism of hydrogen peroxide-induced inhibition of sheep airway cilia. *Am J Respir Cell Mol Biol* 1992;6:667–673.
53. Huszar G, Willetts M, Corrales M. Hyaluronic acid (Sperm Select) improves retention of sperm motility and velocity in normospermic and oligospermic specimens. *Fertil Steril* 1990;54:1127–1134.
54. Kornovski BS, McCoshen J, Kredentser J, Turley E. The regulation of sperm motility by a novel hyaluronan receptor. *Fertil Steril* 1994;61: 935–940.
55. Buch S, Han RN, Cabacungan J, Wang J, Yuan S, Belcastro R, Deimling J, Jankov R, Luo X, Lye SJ, *et al.* Changes in expression of platelet-derived growth factor and its receptors in the lungs of newborn rats exposed to air or 60% O(2). *Pediatr Res* 2000;48:423–433.